Supporting Information

Synthesis of 2D/3D Carbon Hybrids by Heterogeneous Space-Confined Effect for Electrochemical Energy Storage†

Shan Zhu[a,1], Kui Xu[b,1], Simi Sui[a,1], Jiajun Li[a], Liying Ma[a,], Chunnian He[a,c,d], Enzuo Liu[a,c], Fang He[a], Chunsheng Shi[a], Ling Miao[b], Jianjun Jiang[b], and Naiqin Zhao[a,c,d,*]*

[a] School of Materials Science and Engineering and Tianjin Key Laboratory of Composites and Functional Materials, Tianjin University, Tianjin 300350, China

[b] School of Optical and Electronic Information, Huazhong University of Science and Technology, Wuhan 430074, China

[c] Collaborative Innovation Center of Chemical Science and Engineering, Tianjin 300350, China

[d] Key Laboratory of Advanced Ceramics and Machining Technology, Ministry of Education, Tianjin, 300350, China

[*]Corresponding authors: E-mail: nqzhao@tju.edu.cn; lyma@tju.edu.cn

[1]These authors contribute equally to this work.

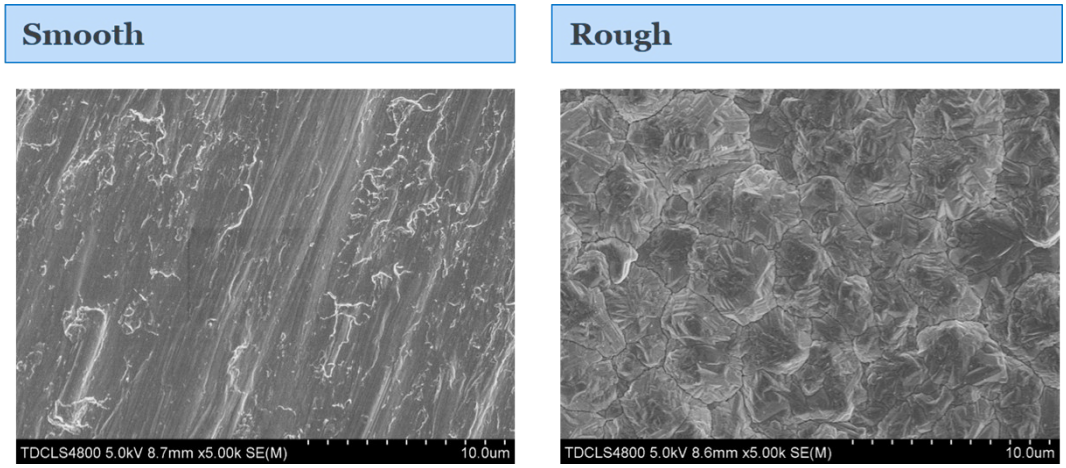

Figure S1. (a) The smooth surface of Cu foil, which can not remain the precursor solution. (b) The rough surface of Cu foil, which can be used for producing N-GPC.

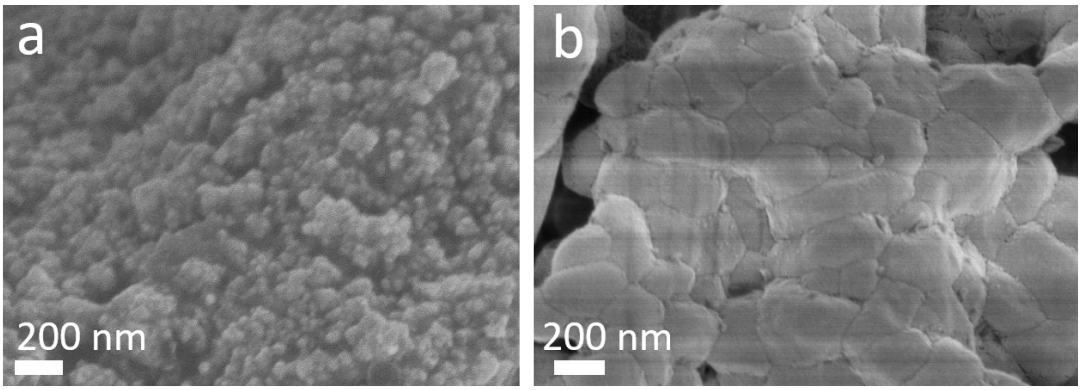

Figure S2. The carbon-coated salt particles of (a) N-GPC and (b) N-PC.

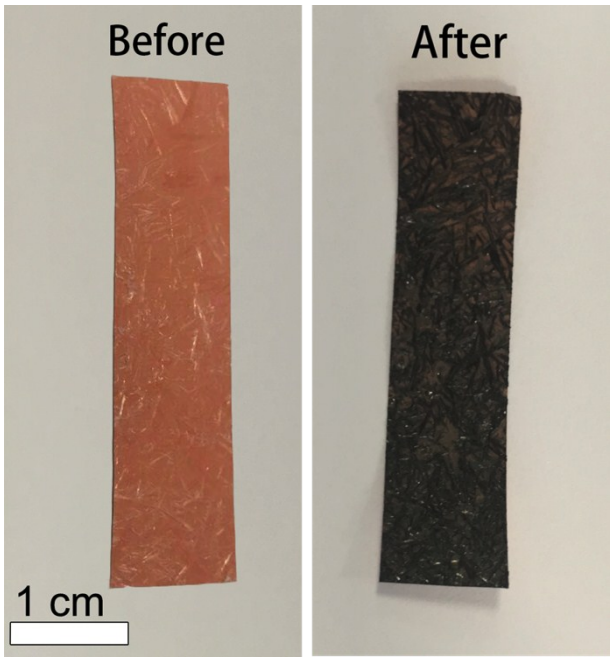

Figure S3. The optical images of the coated Cu foil (4 × 1 cm^2) before and after the calcination.

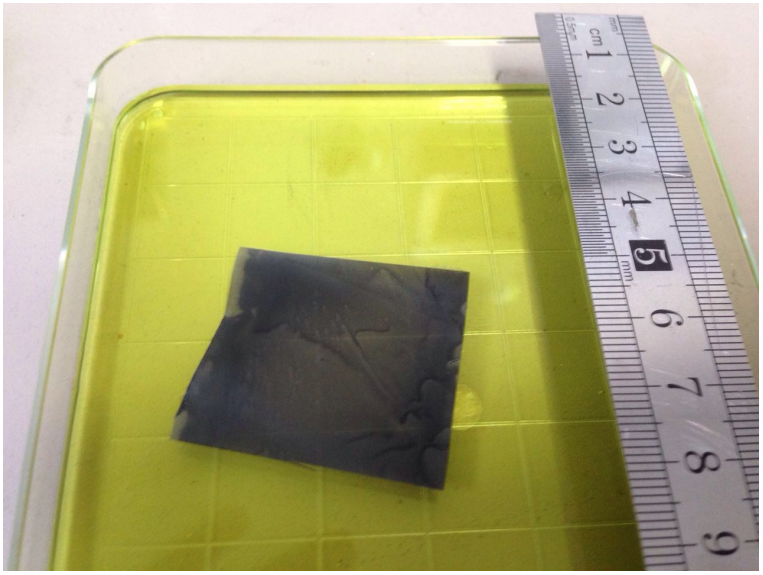

Figure S4. The optical image of free-standing N-GPC floating on the $FeCl_3$-HCl solution.

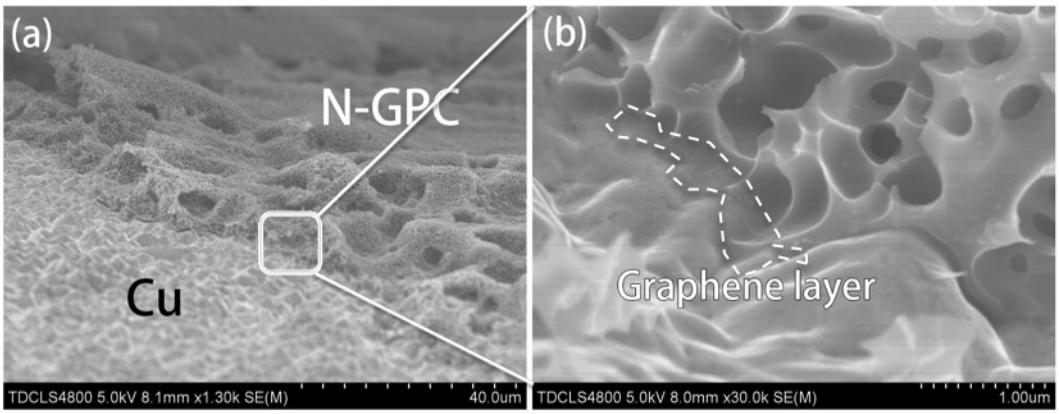

Figure S5. The SEM images: cross view of sandwich-like structure (N-GPC/Graphene/Cu).

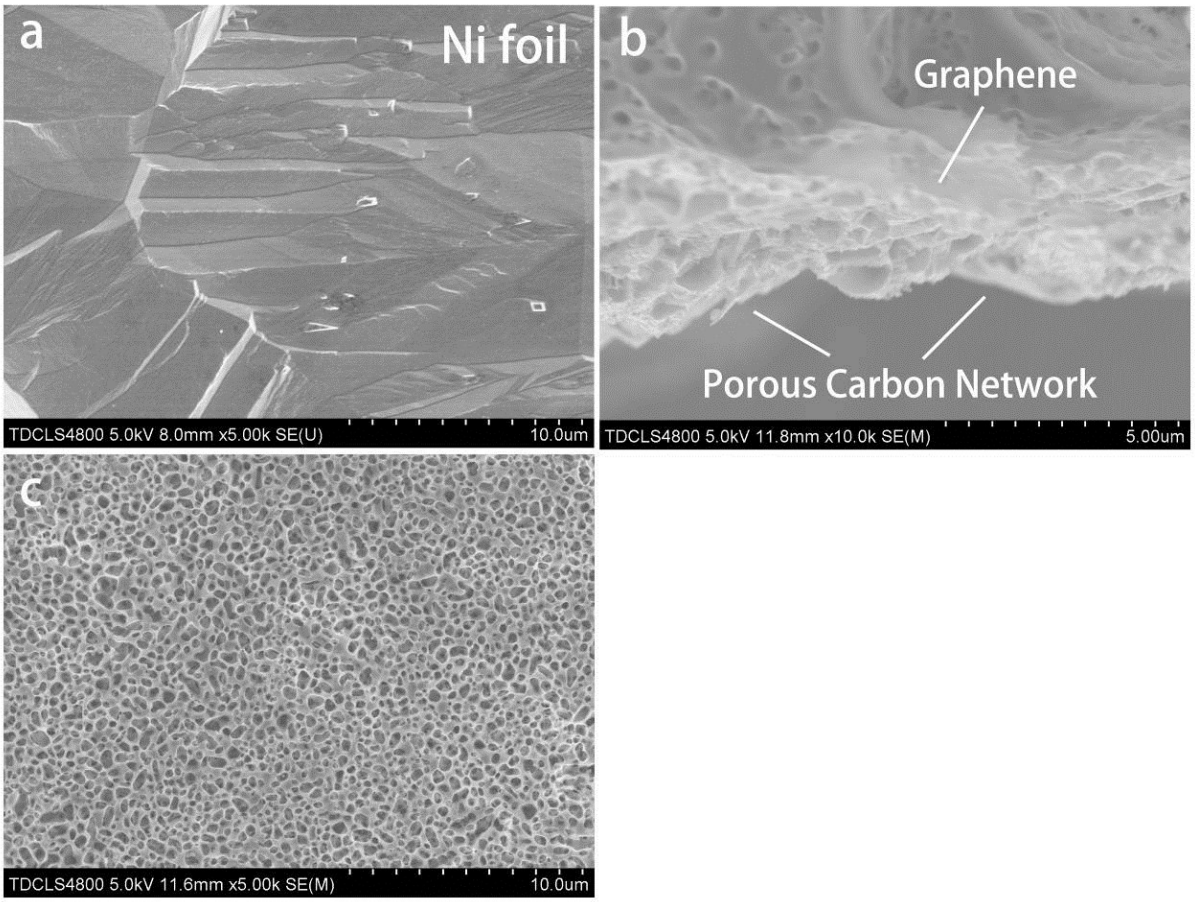

Figure S6. The SEM images of (a) Ni foil; (b) profile view and (c) top view of N-GPC based on Ni substrate.

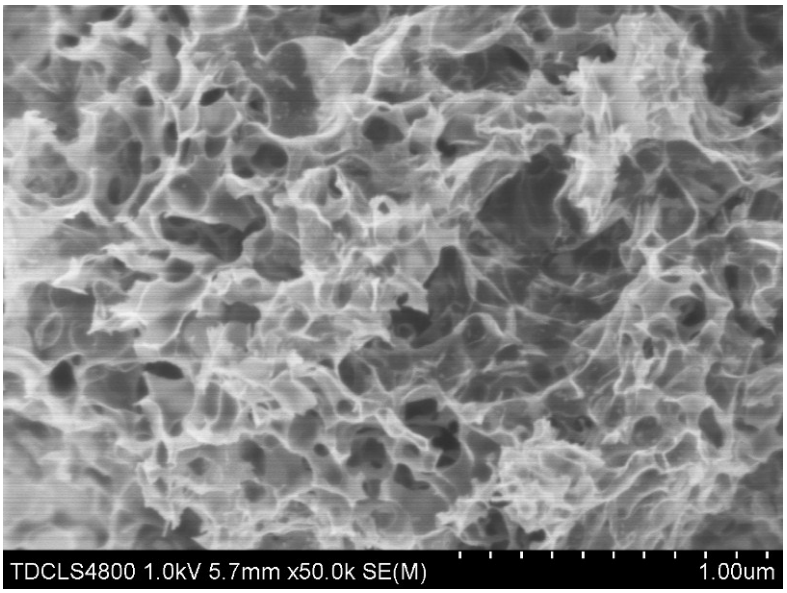

Figure S7. The SEM image of N-PC.

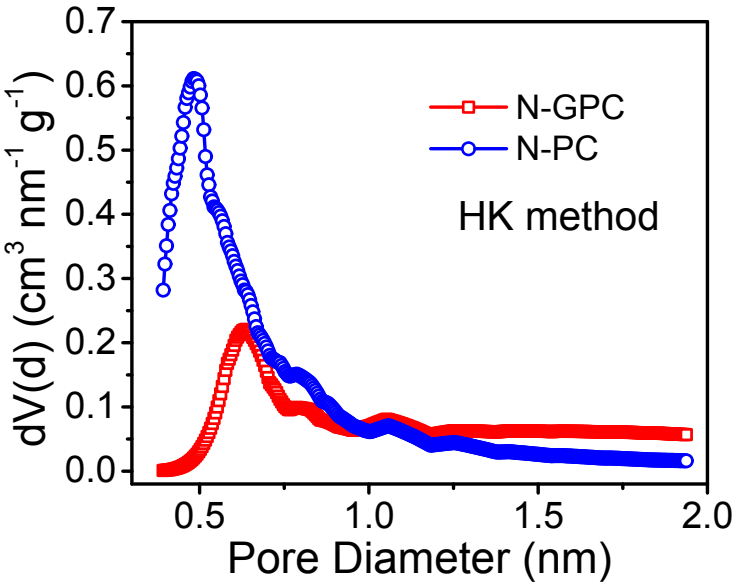

Figure S8. The micropores size distribution analysis based on HK method of N-GPC and N-PC.

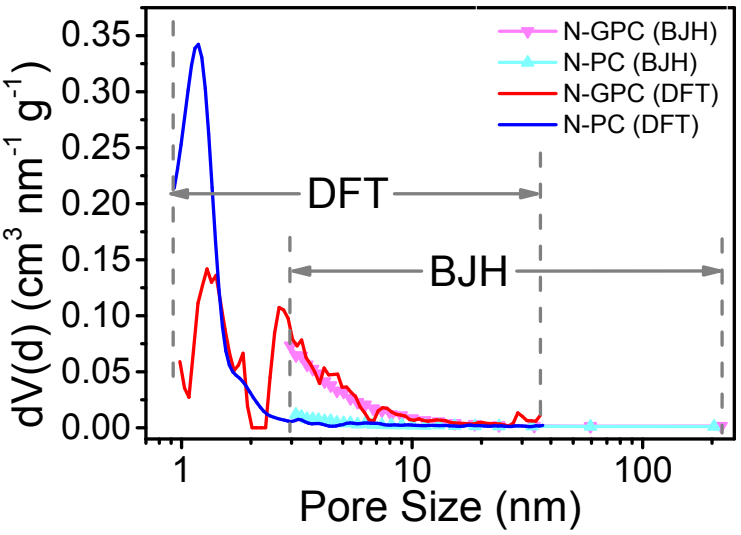

Figure S9. Pore size distribution analysis combining the DFT and BJH theories.

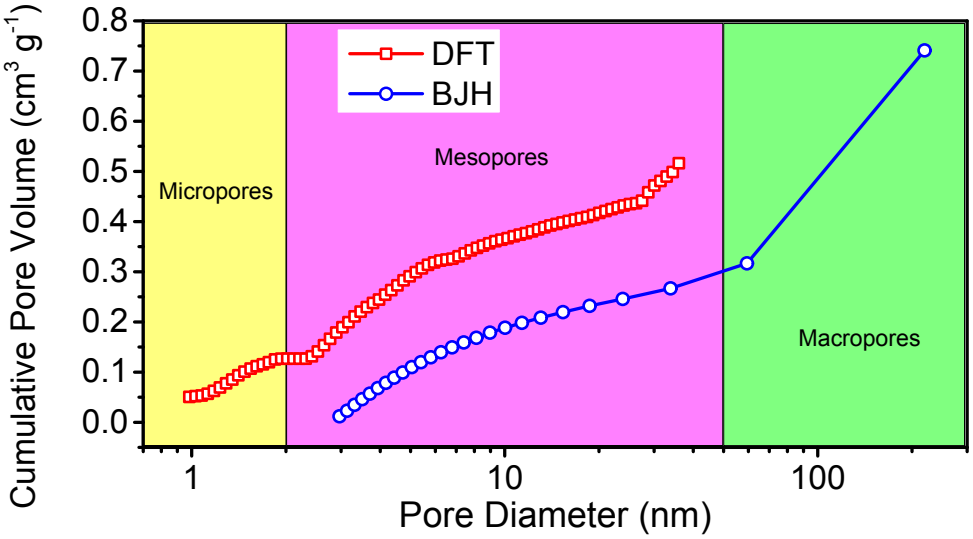

Figure S10. The cumulative pore volumes of N-GPC based on DFT and BJH method.

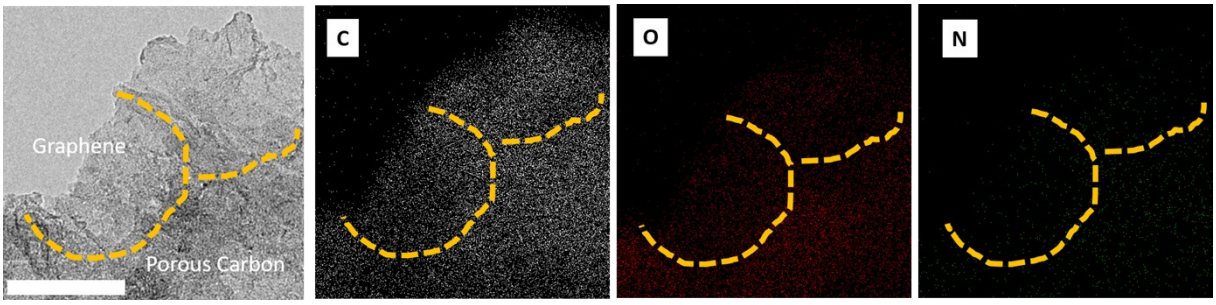

Figure S11. The EDS mapping of N-GPC. The orange line indicates the outline of 3D porous carbon.

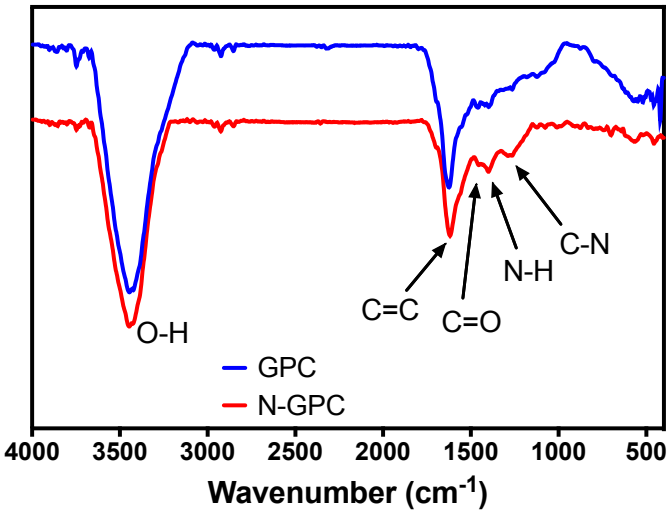

Figure S12. FTIR results of N-GPC and GPC.

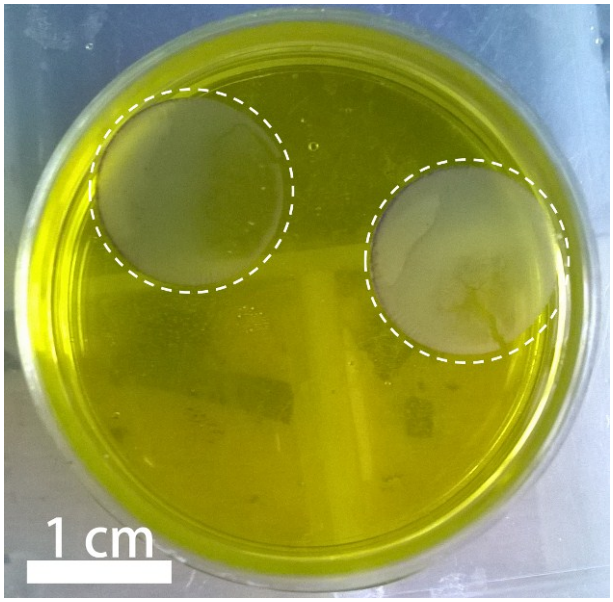

Figure S13. The optical image of wave-like graphene.

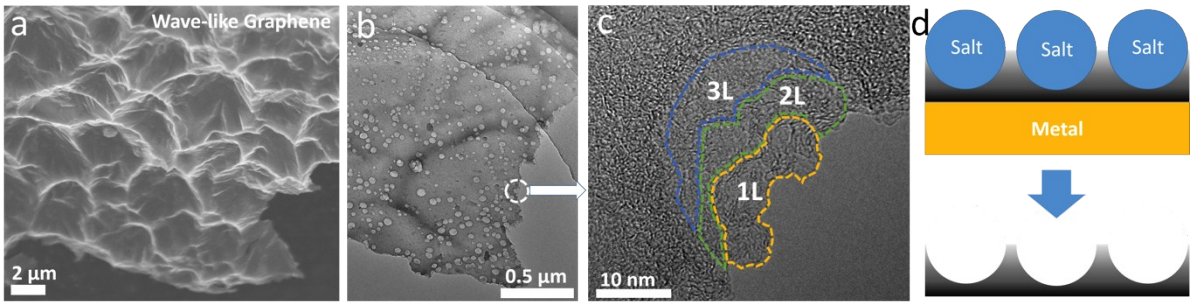

Figure S14. (a) SEM and (b) TEM image and (c) enlarged edge part of wave-like graphene; (d) schematic illustration of heterogeneous space-confined effect for fabricating of wave-like graphene.

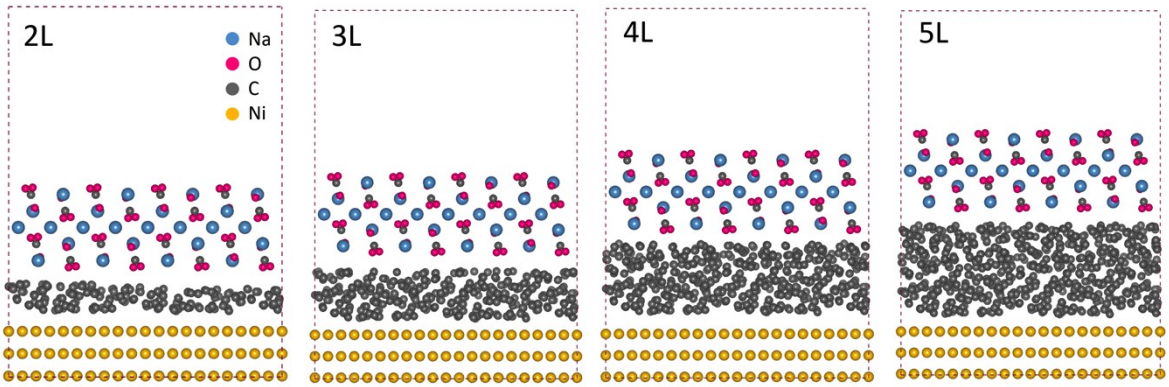

Figure S15. The models of 2, 3, 4, 5 layers of carbon with the Na_2CO_3 confine.

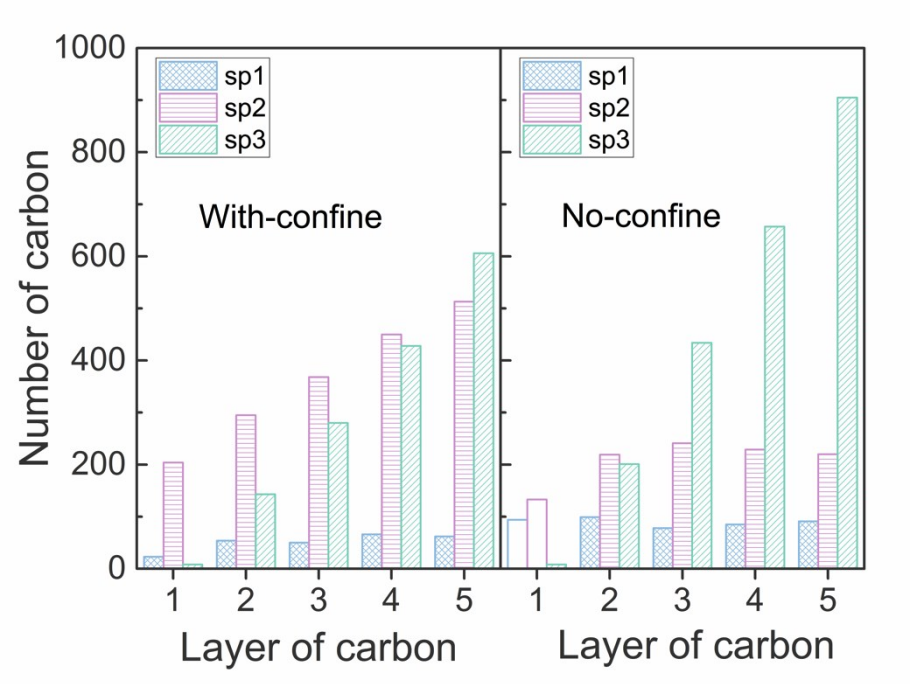

Figure S16. The number of sp^1, sp^2 and sp^3 type carbon for 1-5 layers.

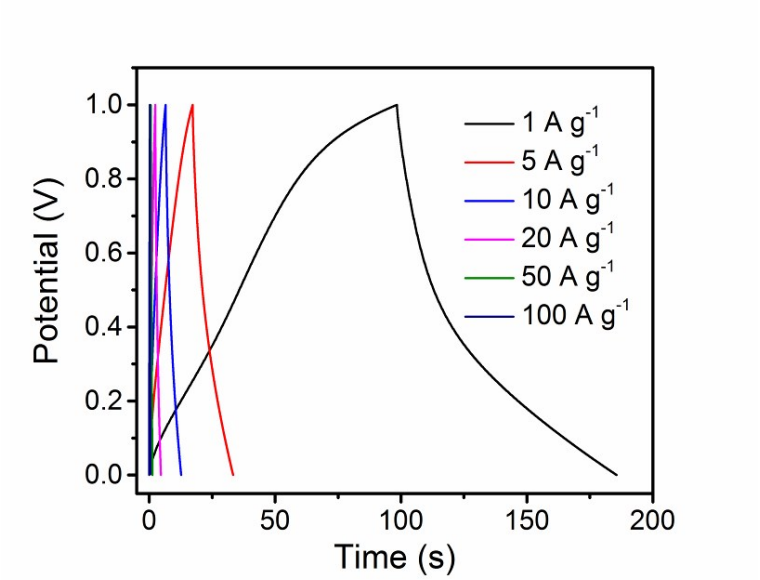

Figure S17. The galvanostatic charging/discharging curves of N-PC powder at various current densities.

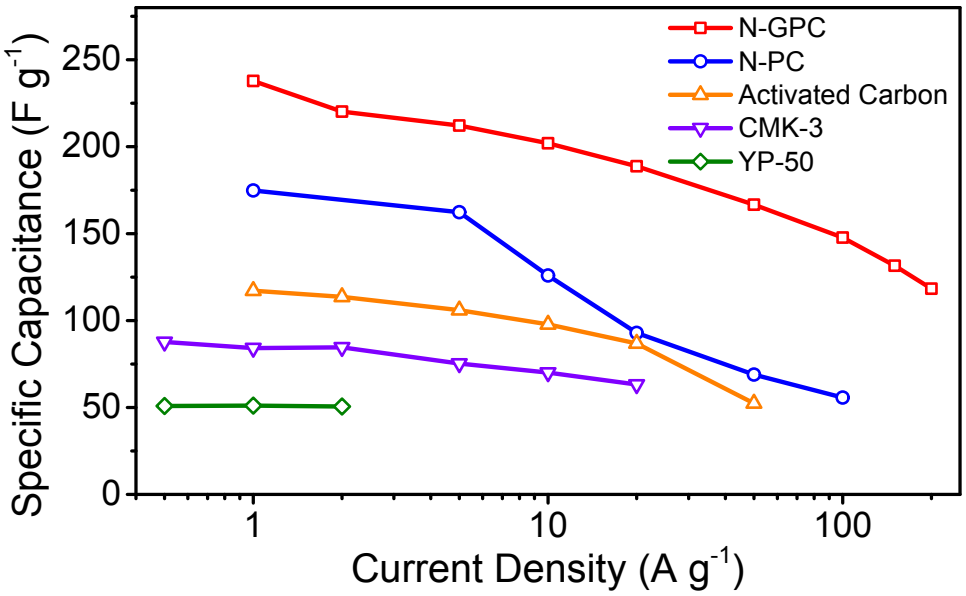

Figure S18. The capacitive performances of various carbon materials. The reference samples are the typical commercial carbon, including YP-50F (Kuraray Chemical. Co., Japan), CMK-3 (Nanjing XFNANO Materials Tech Co., China) and Activated carbon (Lision Technology Inc., China), which are treated as the process of N-PC to act as the electrode of supercapacitor.

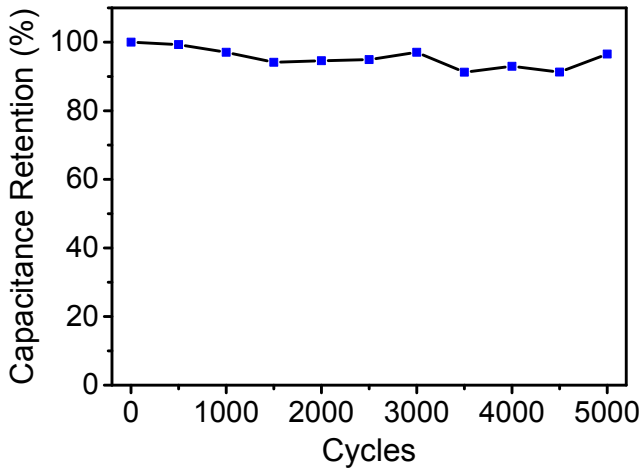

Figure S19. The cycling stability of N-GPC, which is tested at 5 A g^{-1} for 5000 cycles.

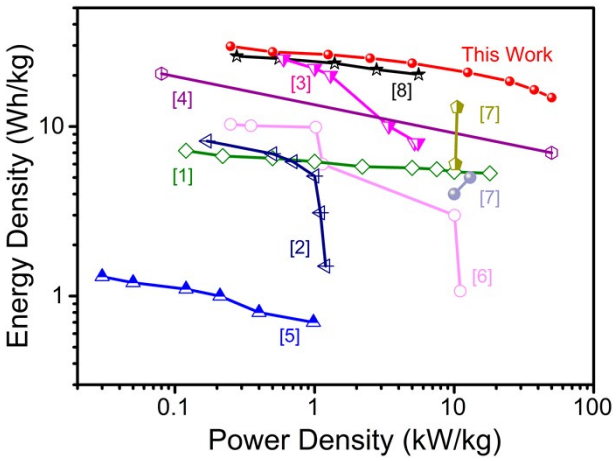

Figure S20. Ragone plot of N-GPC and other reported materials.

Table S1. The SSA, micropores, mesopores and macropores volumes of N-GPC and N-PC

	SSA (m^2 g^{-1})	Micropores Volume (cm^3 g^{-1})	Mesopores Volume (cm^3 g^{-1})		Macropores Volume (cm^3 g^{-1})
N-GPC	498.5	0.127	0.389 (DFT)	0.316 (BJH)	0.425
N-PC	665.0	0.230	0.113 (DFT)	0.121 (BJH)	0.283

[#]The mesopores volumes are calculated by both of DFT and BJH methods.

Table S2. The XPS details of N-GPC, N-PC and GPC

	C (at. %)	O (at. %)	N (at. %)	Other[#] (at. %)
N-GPC	79.3	15.93	4.11	0.65
N-PC	81.56	11.88	5.82	0.73
GPC	92.21	7.45	0	0.34

[#]The other elements include Na, Fe and Cl, which are derived from the salt template or the residual etching solution.

Table S3. The performances of several carbon-based electrode materials

Sample	Lithium ion battery		Supercapacitor		Ref
	Capacitance (mAh g^{-1})	Test Condition	Capacitance (F g^{-1})	Test Condition	
This work	775	0.1 A g^{-1}	238	1 A g^{-1}	
N-GPC			118	200 A g^{-1}	
Graphene-CNTs hybrid materials	458	74.4 mA g^{-1}			[9]
Graphene-CNTs hybrid papers	330	100 mA g^{-1}			[10]
Graphitized boron-doped carbon foam	310	20 cycles			[11]
Hybrid carbon nanotube and graphene nanostructures	370	1.5 A g^{-1}			[12]
MOF-derived N-doped porous carbon	2163	0.1 A g^{-1}			[13]
N-doping graphene	798	0.5 A g^{-1}			[14]
Graphene-carbon nanotube hybrid materials			230	0.01 Hz	[15]
Graphene-single-walled carbon nanotube hybrid			350	0.1 A g^{-1}	[16]
3D graphene and carbon nanotube foam			286	1.78 mA cm^{-2}	[17]
Graphenated carbon nanotube			~100	1 mA cm^{-2}	[18]
Graphene/PANI			409	2 A g^{-1}	[19]
Edge-enriched graphene quantum dots			236	0.5 A g^{-1}	[20]

References

1. L.F. Chen, X.D. Zhang, H.W. Liang, M. Kong, Q.F. Guan, P. Chen, Z.Y. Wu, S.H. Yu, ACS Nano, 2012, 6, 7092-7102.

2. Z.S. Wu, A. Winter, L. Chen, Y. Sun, A. Turchanin, X. Feng, K. Müllen, Adv. Mater., 2012, 24, 5130-5135.

3. L. Zhao, L.Z. Fan, M.Q. Zhou, H. Guan, S. Qiao, M. Antonietti, M.M. Titirici, Adv. Mater., 2010, 22, 5202-5206.

4. Z. Xu, Z. Li, C.M.B. Holt, X. Tan, H. Wang, B.S. Amirkhiz, T. Stephenson, D. Mitlin, J. Phys. Chem. Lett., 2012, 3, 2928-2933.

5. S.Y. Wang, B. Pei, X.S. Zhao, R.A.W. Dryfe, Nano Energy, 2013, 2, 530-536.

6. S.H. Aboutalebi, R. Jalili, D. Esrafilzadeh, M. Salari, Z. Gholamvand, S.A. Yamini, K. Konstantinov, R.L. Shepherd, J. Chen, S.E. Moulton, ACS Nano, 2014, 8, 2456-2466.

7. H. Wang, Z.W. Xu, A. Kohandehghan, Z. Li, K. Cui, X.H. Tan, T.J. Stephenson, C.K. King'ondu, C.M.B. Holt, B.C. Olsen, J.K. Tak, D. Harfield, A.O. Anyia, D. Mitlin, ACS Nano, 2013, 7, 5131-5141.

8. S. Zhu, J. Li, Q. Li, C. He, E. Liu, F. He, C. Shi, N. Zhao, Electrochim. Acta, 2016, 212, 621-629.

9. S. Chen, W. Yeoh, Q. Liu, G. Wang, Carbon, 2012, 50, 4557.

10. Y. Hu, X. Li, J. Wang, R. Li, X. Sun, J. Power Sources, 2013, 237, 41.

11. E. Rodríguez, I. Cameán, R. García, A.B. García, Electrochimica Acta, 2011, 56, 5090.

12. W. Wang, I. Ruiz, S. Guo, Z. Favors, H.H. Bay, M. Ozkan, Nano Energy, 2013, 3, 113-118.

13. F. Zheng, Y. Yang, Q. Chen, Nature Commun., 2014, 5, 5261.

14. T. Hu, X. Sun, H. Sun, G. Xin, D. Shao, C. Liu, J. Lian, Phys. Chem. Chem. Phys., 2014, 16, 1060.

15. B. Brown, B. Swain, J. Hiltwine, D.B. Brooks, Z. Zhou, J. Power Sources, 2014, 272, 979.

16. Y. Wu, T. Zhang, F. Zhang, Y. Wang, Y. Ma, Y.Y. Huang, Liu, Y. Chen, Nano Energy, 2012, 1, 820.

17. W. Wang, S. Guo, M. Penchev, I. Ruiz, K.N. Bozhilov, D. Yan, M. Ozkan, C. Ozkan, Nano Energy, 2013, 2, 294.

18. B. Brown, I.A. Cordova, C.B. Parker, B.R. Stoner, J.T. Glass, Chem. Mater., 2015, 27, 2430.

19. M. Hassan, K.R. Reddy, E. Haque, S.N. Faisal, S. Ghasemi, A.I. Minett, V.G. Gomes, Compos. Sci. Technol., 2014, 98, 1.

20. M. Hassan, E. Haque, K.R. Reddy, A.I. Minett, J. Chen, V.G. Gomes, Nanoscale, 2014, 6, 11988.